Numerical Analysis of Nano-imprinting Process Based on Continuum Hypothesis

H. C. Kim*, Y. S. Woo*, W. I. Lee*, S. I. Oh* and B. S. Kim**

*School of Mechanical and Aerospace Engineering, Seoul National University, Korea
sesese72@snu.ac.kr, yswoo72@snu.ac.kr, wilee@snu.ac.kr, sioh@snu.ac.kr
**Korea Institute of Machinery and Materials, Changwon, Kyungnam, Korea
kbs@kimm.re.kr

ABSTRACT

Nano-imprint lithography (NIL) is a processing technique capable of transferring nano-scale patterns onto a thin film of thermoplastics such as polymethyl methacrylate (PMMA). Feature sizes down to 10 nm have been demonstrated to be made possible using this process. In NIL, it is imperative to thoroughly understand the flow of resin to ensure complete transfer of the pattern. Due to the size of the pattern, experimental observation may be very difficult, if not totally impossible. In this study, a numerical simulation tool to calculate the two dimensional resin flows and heat transfer during NIL has been developed. The code is based on the continuum hypothesis with some modification to accommodate the size effect, such as slip along the boundary. In order to fully account for the surface tension effect, which may play a dominant role, a moving grid system is adopted. Numerical simulations have been performed for different sets of process parameters. Parametric study shows that the surface tension effect indeed is a dominant factor. With change in the values of the surface tension as well as the contact angle, filling patterns and the resulting free surface become different.

Keywords: Nanoimprint, Surface tension effect, Slip, Numerical simulation

1 INTRODUCTION

There are different fabrication methods available for the production of nanostructures. Optical lithography technique, which is widely used in semiconductor industry, is limited by the light diffraction at nano length scale. Electron beam and scanning probe microscope (SPM) lithographies suffer from low productivity while the X-ray lithography requires a major capital investment. The nanoimprint lithography (NIL) is known as a low cost alternative to these methods of fabricating nano-scale patterns as small as 10nm [1].

The NIL process consists of four stages, namely spin coating, embossing, de-molding and dry etching (Fig. 1). As the structures become smaller and more complex, it is very important to understand the behavior of thin polymer film during embossing and de-molding process. Due to the size of the pattern, experimental observation may be very difficult. Therefore, numerical simulation may serve as a viable and useful tool to design and optimize the processing conditions [2].

There are two ways to simulate nano scale flows, namely top-down and bottom-up approaches. In the top-down approach, it is assumed that the polymeric melt flow is a continuum. On the contrary, the bottom-up approach employs the molecular dynamics (MD) technique.

Even though the bottom-up approach may provide more accurate details of the polymer melt behavior, comprehensive modeling is not yet available. Moreover, calculation overhead is still prohibitively large. Therefore, as a practical consideration, the top down approach was used in this study. For the numerical analysis, two dimensional moving grid system was chosen to obtain the accurate prediction of the flow front. Numerical mesh was regenerate at every time step. Effects of surface tension as well as the slip at the boundary were also considered.

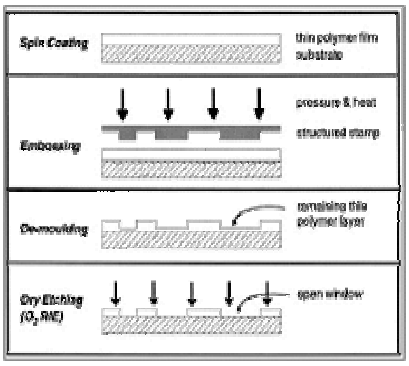

Figure. 1 NIL Process

2 CONTINUUM MODEL

Behavior of polymer melt during NIL process can be obtained by solving the following the continuity, momentum and energy conservation equations [3].

Mass conservation equation:

$$\frac{D\rho}{Dt} + \rho \nabla \cdot u = 0 \tag{1}$$

Momentum conservation equation:

$$\rho \frac{Du}{Dt} = \nabla \cdot \sigma + \rho f \tag{2}$$

where $\sigma = -PI + 2\mu D$

Energy conservation equation:

$$\rho C_v \frac{DT}{Dt} = -\nabla \cdot q + Q \tag{3}$$

In the above equations, *t* is time, *u* is the velocity, ρ is density, μ is the dynamic viscosity, *f* is the body force and σ denote the stress.

The penalty function method was employed to solve the above equations. Using this method, Eq.(1) and (2) can be reformulated into a single equation by expressing pressure in terms of velocity as follows [4]

$$P = -\gamma_e \nabla \cdot u \tag{4}$$

where γ_e is a penalty parameter.

2.1 Surface Tension Modeling

Surface tension is usually neglected in macro-scale analysis. However, in NIL, surface tension may play a dominant role due to the size effect.

The surface stress boundary condition at an interface between two fluids is given as [5]

$$(p_1 - p_2 + \sigma\kappa)\vec{n}_i = (\tau_{1ik} - \tau_{2ik})\vec{n}_k + \frac{\partial \sigma}{\partial x} \tag{5}$$

where σ is the fluid surface tension coefficient, p_α is the pressure in fluid α for $\alpha = 1, 2$, is the viscous stress tensor, $\tau_{\alpha ik}$ is the unit normal at the interface and κ is the local surface curvature(=$-(\nabla \cdot \vec{n}) = 1/R$).

Assuming that the viscous effect neglected on a free surface and the fluid is incompressible, we can rearrange the surface boundary condition constant σ as follows [5]

$$p_s \equiv p_2 - p_1 = \sigma\kappa \tag{6}$$

2.2 Wall Adhesion

Effect of wall adhesion at fluid interface can be estimated in terms of the contact angle between cavity wall and free surface. The static contact angle is not simply a material property of the fluid. It depends on the smoothness and geometry of the wall as well.

For still fluids, the normal vector to the interface for calculating the curvature at boundary points can be expressed using the unit normal to the interface at points on the wall as follows [6]

$$\vec{n} = \vec{n}_w \cos\theta_{eq} + \vec{n}_t \sin\theta_{eq} \tag{7}$$

where θ_{eq} is the contact angle between the interface and the wall, $\vec{n}_t$ lies in the wall and is the unit normal to the contact line and $\vec{n}_w$ is the unit wall normal directed into the wall.

Wall adhesion boundary condition becomes more complicated when the contact line is in motion. In NIL, because the stamp wall moves downward, the dynamic contact angle was used instead of the static contact angle to estimate the velocity effect on the contact angle [7].

$$v = \frac{\sigma}{\pi} \frac{-\frac{\bar{\mu}}{\mu}(\sin^2\theta_d - \theta_d^{\,2}) + \sin^2\theta_d - \theta_d(\theta_d + \pi)}{(\mu - \bar{\mu})\sin^2\theta_d} (\cos\theta_d - \cos\theta_s) \tag{8}$$

where θ_s is the static contact angle, θ_d is the dynamic contact angle, v is velocity near the contact point, μ is the fluid viscosity and $\bar{\mu}$ is the air viscosity.

2.3 Slip Boundary Condition

In macroscopic flow, the no-slip condition at a fluid-solid interface is enforced. However, in nano-scale, it is known that slip takes place between the fluid and the contact wall. For both liquids and gases, the following Navier boundary condition empirically relates the tangential velocity slip at the wall to the local shear [8].

$$\Delta u\big|_w = u_{fluid} - u_{wall} = L_s \frac{\partial u}{\partial y}\bigg|_w = L_s \dot{\gamma} \tag{9}$$

where L_s is the constant slip length and $\dot{\gamma}$ is the strain rate estimated at the wall. The slip length for nano-scale fluid can be defined using Lennard-Jones potential model as follows [9]

$$L_s = L_s^0 \left[1 - \frac{\dot{\gamma}}{\dot{\gamma}_c}\right]^{-\frac{1}{2}}, \quad \dot{\gamma}_c^{-1} \approx \tau^{wf} = \left(\frac{m\sigma^{wf}}{\varepsilon^{wf}}\right)^{\frac{1}{2}} \tag{10}$$

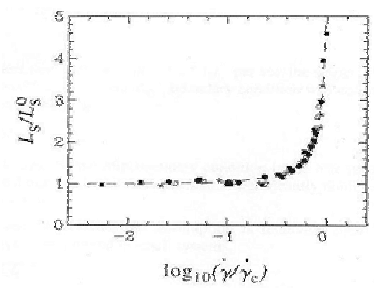

Figure. 2 Slip length as a function of shear rate

where τ^{wf} is the characteristic time, σ^{wf} is length of wall-fluid coupling, ε^{wf} is the strength of wall-fluid coupling and m is mass of a molecule. L_s^0 ranges from 0 to 17 σ^{wf}. Relationship between the slip length and the shear rate is shown in Fig. 2.

2.4 Rheological behavior of polymeric melts

The viscosity of polymeric melts changes according to the shear rate. To describe this shear rate dependency of viscosity, the Cross Williams-Lendal-Ferry (WLF) model was used [10].

3 VALIDATION AND RESULTS

3.1 Validation

In order to validate the numerical code, mesh size sensitivity was evaluated. Identical flow front shapes were obtained independent of mesh size for the same process conditions.

3.2 Result

To simplify numerical studies, we assumed that polymeric melt is incompressible. The stamp moves down with a constant velocity, and the density of PMMA is 1.17×10^3 kg/m^3. The geometry of the stamp and PMMA layer is shown in Fig. 3.

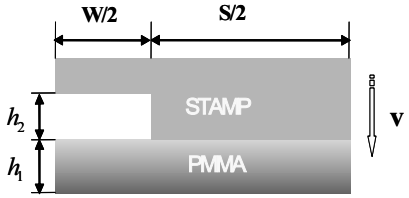

Figure. 3 Geometry of stamp and PMMA layer

First, calculation was done for the no-slip boundary condition without surface tension. These conditions are the ones encountered in the most macroscopic flow simulations. Calculated flow front shape is shown in Fig.4. The geometry considered was as follows: S=500nm, W=100nm, h_1=70nm, h_2=50nm and v=0.2nm/s. The temperature of the stamp as well as the PMMA layer was taken to be 150℃.

Figure. 4 Flow front shape at t=20 sec. Simulated result for no slip boundary condition without surface tension.

In order to evaluate the effect of slip length, calculations were done for different values of slip length ranging from 0.01nm to 0.1nm. Geometry and process conditions were same as the previous example. Surface tension was also considered (θ_s =30°, and σ = 30mN/m). Numerical simulations were performed for two different cases, L_s^0=0.01nm and L_s^0=0.1nm. Even though the results were not identical as shown Fig. 5, the effect of slip length on the change in the flow front shape was found to be minimal.

(a) The case of L_s^0=0.01nm

(b) The case of L_s^0=0.1nm

Figure. 5 Effect of slip length on the flow front shape at t=20 sec.

To study the effect of temperature, three different cases were considered for 140℃, 150℃ and 160℃. In these cases, different geometry was used as follows: S=100nm, W=300nm, h_1=150nm, h_2=50nm, v=3nm/s. Parameters for the surface tension and the slip at the boundary were given as θ_s =30°, σ =30mM/m and L_s^0=0.1nm. As can be seen from Fig.6, increase in the temperature resulted in completely different filling patterns. This change in the filling pattern is attributable to the decrease of viscosity with temperature increase. At lower viscosity of PMMA, the effect of surface tension and slip length became relatively larger than the shear stress caused by the viscosity. Therefore, the flow tends to rise faster along the boundary resulting in a depression in the center (Fig.6c).

(a) T=140℃

(b) T=150℃

(c) T=160℃

Figure. 6 Effect of temperature on the flow front shape at t=6 and 12 sec.

For the same geometry, effect of the stamp velocity was also investigated. The process temperature was set to be T=140℃. Two different stamp velocities were considered, v =3nm/s and 1nm/s. As the stamp velocity is decreased, contribution of surface tension to drive the flow becomes more important. Therefore, as can be seen in Fig. 7, the flow front near the stamp wall rose faster.

(a) v=3nm/s (filling time=13s) at t=6, 12 sec

(b) v=1nm/s (filling time=39s) at t=18, 36 sec

Figure. 7 Effect of stamp velocity on the flow front shape

Finally, we compared the flow front shape for the change of the surface tension coefficient. Same geometry was used as the last two examples. Temperature was 140℃ and the stamp velocity was 3nm/s. As the surface tension coefficient becomes larger, the surface tension and capillary force increase. Thus with increased surface tension, flow front near the border ascended faster as shown Fig. 8.

(a) σ =30mN/m at t=6, 12 sec

(b) σ =60mN/m at t=6, 12 sec

Figure. 8 Effect of surface tension coefficient σ on the flow front shape at t=6 and 12 sec.

4 CONCLUSION

Nano-scale flow arising in NIL process was simulated using a code based on continuum hypothesis. In order to account for the size effect, surface tension and the slip length were included in the numerical modeling. Effect of parameters such as the temperature, the stamp velocity, the slip length and the surface tension coefficient were investigated. It was shown that the change in these parameters resulted in different evolution of flow front pattern. The code developed in this study can be used in optimizing the process variables in NIL.

REFERENCES

[1] S. Chou et al., 1996, "Imprint lithography with 25 nanometer resolution", *Science*, Vol. 272, pp.85-87.

[2] L.J. Heyderman et al., 2000, "Flow behaviour of thin polymer films used for hot embossing lithography", *Micro electronic Engineering*, Vol. 54, pp.229-245.

[3] L. D. Landau and E.M. Lifshitz, 1959, Fluid Mechanics, Pergamon, New York.

[4] J.N. Reddy and D.K. Gartling, 1994, The Finite Element Method in Heat Transfer and Fluid Dynamics, CRC Press.

[5] J. U. Brackbill et al., 1992, "A continuum method for modeling surface tension", *Journal of Computational Physics*, Vol. 100, pp.334-354.

[6] Jun-Ho Jeong et al., 2002, "Flow Behavior at the Embossing Stage of Nanoimprint Lithography", *Fiber and Polymer 2002*, Vol. 3, No3, pp.113-119.

[7] Arian Novruzi et al., 2003, "An analytical study on the dynamical contact angle of a drop in steady state motion", Department of Mathematics and Statistics, University of Ottawa, Canada.

[8] Mohamed Gad-el-Hak, 2001, "Flow physics in MEMS", *Mec. Ind.* , Vol. 2, pp.313-341.

[9] Thompson P.A., Troian S.M., 1997, "A general boundary condition for liquid flow at solid surfaces", *Phys. Rev. Lett,*, Vol. 63, pp. 766-769.

[10] Ferry J.D., 1989, Viscoelastic Properties of Polymers, John Wiley& Sons